

17. S. M. Burgess, N. Kleckner, *Genes Dev.* **13**, 1871 (1999).
18. D. Zickler, N. Kleckner, *Annu. Rev. Genet.* **32**, 619 (1998).
19. ———, *Annu. Rev. Genet.* **33**, 603 (1999).
20. R. Padmore, L. Cao, N. Kleckner, *Cell* **66**, 1239 (1991).
21. N. Hunter, N. Kleckner, *Cell* **106**, 59 (2001).
22. O. Kratky, G. Porod, *Rec. Trav. Chim.* **68**, 1106 (1949).
23. P. J. Flory, *Statistical Mechanism of Chain Molecules* (Wiley, New York, 1969).
24. K. Rippe, P. H. von Hippel, J. Langowski, *Trends Biochem. Sci.* **20**, 500 (1995).
25. L. Ringrose, S. Chabanis, P. O. Angrand, C. Woodrooffe, A. F. Stewart, *EMBO J.* **18**, 6630 (1999).
26. K. Rippe, *Trends Biochem. Sci.* **26**, 733 (2001).
27. P. Hahnfeldt, J. E. Hearst, D. J. Brenner, R. K. Sachs, L. R. Hlatky, *Proc. Natl. Acad. Sci. U.S.A.* **90**, 7854 (1993).
28. S. E. Gerchman, V. Ramakrishnan, *Proc. Natl. Acad. Sci. U.S.A.* **84**, 7802 (1987).
29. K. E. van Holde, *Chromatin* (Springer, Heidelberg, 1989).
30. The flexibility of chromatin in higher eukaryotes is not firmly established. FISH analysis of mammalian chromosomes yielded values of  $l$  [ $l = 137$  to  $440$  nm (27) and  $l = 196$  to  $272$  nm (42)], whereas detailed in vitro experiments with single chromatin fibers from chicken erythrocytes yielded lower values of  $l$  [ $l = 60$  nm (43)].
31. The local concentration is maximal for sites separated by  $\sim 1.7$  times the statistical segment length  $l$ . We estimate that the contour length of the yeast chromatin fiber is 11.1 nm/kb. A segment length of 56 to 69 nm (as determined in Fig. 3, A and B) will then correspond to 5.0 to 6.2 kb. The local concentration is therefore maximal for sites separated by 8.5 to 10.5 kb.
32. P. B. Moens, R. E. Pearlman, *Bioessays* **9**, 151 (1988).
33. Y. Blat, N. Kleckner, *Cell* **98**, 249 (1999).
34. S. Laloraya, V. Guacci, D. Koshland, *J. Cell Biol.* **151**, 1047 (2000).
35. P. M. Sharp, A. T. Lloyd, *Nucleic Acids Res.* **21**, 179 (1993).
36. B. Dujon, *Trends Genet.* **12**, 263 (1996).
37. F. Baudat, A. Nicolas, *Proc. Natl. Acad. Sci. U.S.A.* **94**, 5213 (1997).
38. J. L. Gerton et al., *Proc. Natl. Acad. Sci. U.S.A.* **97**, 11383 (2000).
39. G. P. Holmquist, *Am. J. Hum. Genet.* **51**, 17 (1992).
40. Given a table of all distances between  $n + 1$  points, one can find a constellation of  $n + 1$  points in three dimensions, satisfying this distance table, with the use of the following algorithm, which is based on Cholesky decomposition of symmetric matrices. The distance table can be converted to a symmetric  $n \times n$  matrix  $\mathbf{M}$  that contains all the inner products of the  $n + 1$  points in  $n$ -space. If the distance table describes a 3D structure,  $\mathbf{M}$  should have rank 3. In general, however,  $\mathbf{M}$  does not have rank 3 because of noise in the data. By slightly moving  $\mathbf{M}$  in  $n^2$ -space, we obtain a matrix  $\mathbf{M}'$ , close to  $\mathbf{M}$ , which does have rank 3. This is done by setting all but the three largest eigenvalues to zero. Indeed, three eigenvalues we determined were considerably larger than zero, and the other had very low values, which indicates that the  $\mathbf{M}$  is very close to a matrix with rank 3. This is strong support for the accuracy of the distance calculation. Cholesky decomposition of  $\mathbf{M}'$  will yield the positions of the  $n + 1$  points in three dimensions, and the distances between those points will nearly satisfy the experimental distance table. By using  $\mathbf{M}'$  instead of  $\mathbf{M}$  we introduce an error, which is related to the error in the data of the experimental distance table. The distance between  $\mathbf{M}$  and  $\mathbf{M}'$  is a measure for this error and was found to be only about 6%.
41. The FJC model will give a reasonable approximation of  $f_M$  for values of  $s$  larger than 3 to 4 times the statistical segment length, which, for a value of  $l = 56$  to  $69$  nm and a contour length of 11.1 nm/kb, corresponds to 15 to 20 kb. For sites separated by less than 3 but more than 1.7 statistical segments (corresponding to site separation distances of 8.5 to 15 kb), Eq. 3 will yield a value of  $r$  that is slightly too high, but the highest deviation is about 20% (9). Because only 2 of the 78 site separations were smaller than 15 kb (12 and 13 kb), the set of 78 cross-

linking frequencies presented in Fig. 3A could be used to estimate the average spatial distances between the respective sites according to Eqs. 1 and 3 with good accuracy. For  $k$  the chromosome-wide average value of  $4.0 \times 10^6 \text{ M}^{-1}$  was used, which was determined by fitting the chromosome-wide data set to Eq. 2. Because the analysis of AT- and GC-rich domains (Fig. 3B) revealed small local variations in the value of  $k$ , this might introduce small errors (at most 10%) in certain regions of the chromosome.

42. J. Y. Ostashevsky, C. S. Lange, *J. Biomol. Struct. Dyn.* **11**, 813 (1994).
43. Y. Cui, C. Bustamante, *Proc. Natl. Acad. Sci. U.S.A.* **97**, 127 (2000).
44. In some cases a very small amount of ligation product was detected in the absence of cross-linking, but

this was always 5% or less than the amount detected after cross-linking with 1% formaldehyde.

45. We thank Kleckner lab members for discussions. We are especially grateful to J. M. Perry and A. J. M. Walhout for valuable comments on the experiments and the manuscript. Part of the work by K.R. was done at the division "Biophysik der Makromoleküle" of the Deutsches Krebsforschungszentrum in Heidelberg. Supported by EMBO long-term fellowship ALTF-223-1998 and a fellowship from the Medical Foundation/Charles A. King Trust (J.D.), the Volkswagen Foundation program "Junior Research Groups at German Universities" (K.R.), and NIH grants GM44794 and GM25326 (N.K.).

6 November 2001; accepted 16 January 2002

## A Class of Potent Antimalarials and Their Specific Accumulation in Infected Erythrocytes

Kai Wengelnik,<sup>1</sup> Valérie Vidal,<sup>2</sup> Marie L. Ancelin,<sup>1</sup>  
Anne-Marie Cathiard,<sup>1</sup> Jean Louis Morgat,<sup>3</sup> Clemens H. Kocken,<sup>4</sup>  
Michèle Calas,<sup>2</sup> Socrates Herrera,<sup>5</sup> Alan W. Thomas,<sup>4</sup>  
Henri J. Vial<sup>1\*</sup>

During asexual development within erythrocytes, malaria parasites synthesize considerable amounts of membrane. This activity provides an attractive target for chemotherapy because it is absent from mature erythrocytes. We found that compounds that inhibit phosphatidylcholine biosynthesis de novo from choline were potent antimalarial drugs. The lead compound, G25, potently inhibited in vitro growth of the human malaria parasites *Plasmodium falciparum* and *P. vivax* and was 1000-fold less toxic to mammalian cell lines. A radioactive derivative specifically accumulated in infected erythrocytes to levels several hundredfold higher than in the surrounding medium, and very low dose G25 therapy completely cured monkeys infected with *P. falciparum* and *P. cynomolgi*.

The widespread resistance of malaria parasites to most common antimalarials, and cross-resistance to structurally unrelated drugs, emphasize the need for new chemotherapeutic targets (1). When parasitizing red blood cells, the parasite invests heavily in membrane biogenesis, making phospholipid (PL) biosynthesis essential for intraerythrocytic development (2), whereas these activities are absent from mature uninfected erythrocytes (3). Phosphatidylcholine (PC) is the major PL present in infected erythrocytes. It is mainly synthesized from plasma-derived choline by the parasite enzymatic machinery and provides an attractive target for antimalarial chemotherapy (2).

To inhibit PC synthesis in malaria parasites, we designed and synthesized a series of compounds based on their capacity to mimic choline structure (4). They were optimized for in vitro antimalarial activity, and there was a very close correlation between the inhibition of parasite growth in vitro and specific inhibition of parasite PC biosynthesis de novo from choline (5). The compounds do not interfere with other types of PL synthesis, such as that of phosphatidylethanolamine or macromolecules like DNA (5). Toxic activity is highest against mature parasites, when PL synthesis is maximal (5). We hypothesize that the most likely drug target is the choline transporter, either on the surface of the infected erythrocyte or in the plasma membrane of the intracellular parasite (6). Structure-activity relation (SAR) studies revealed the importance of the cationic group volume. Duplication of this group (bisquaternary ammonium salts) separated by a sufficiently long alkyl chain markedly increases antimalarial activity to within the low-nanomolar range (7). This defined the lead compound, G25 [1,16-hexadecamethylenebis(*N*-methylpyrro-

<sup>1</sup>CNRS UMR 5539, CP 107, <sup>2</sup>CNRS UMR 5810, CP 22, Université Montpellier II, Place E. Bataillon, 34095 Montpellier Cedex 5, France. <sup>3</sup>CRBA CNRS UMR 5473, Université Montpellier I, Faculté de Pharmacie, 15 Av. Charles Flahault, 34060 Montpellier, France. <sup>4</sup>Department of Parasitology, Biomedical Primate Research Centre, Postbox 3306, 2280 GH Rijswijk, Netherlands. <sup>5</sup>Fundacion Centro de Primates, Universidad del Valle, Cali, Colombia.

\*To whom correspondence should be addressed. E-mail: vial@univ-montp2.fr

## REPORTS

lidinium) dibromide] (7), which we analyze here.

G25 was assessed against *Plasmodium falciparum* strains with preexisting resistance against chloroquine (CQ), quinine (Q), mefloquine, and pyrimethamine (8, 9) and against four clinical isolates with varying resistance to CQ, Q, and cycloguanil from patients in different African countries (10). G25 was effective against all strains and isolates tested, with 50% inhibitory concentrations ( $IC_{50}$ 's) ranging between 1 and 5.3 nM. Steep dose-response curves with  $IC_{90}/IC_{50}$  ratios of less than 3 were consistently observed (9), indicating inhibition of a specific target and not a general cytotoxic effect. To assess the effect of G25 in the host, we measured  $IC_{50}$  levels of G25 against Jurkat lymphoblast, U937 macrophage, and MEG-01 megakaryoblast human cell lines (9). The  $IC_{50}$  obtained was three to four orders of magnitude higher than the  $IC_{50}$  against *P. falciparum*. No mutagenic activity [Ames test (11)] with or without metabolic activation was evident at the highest nontoxic concentration (77  $\mu$ M).

Antimalarial activity [4 days suppressive test (12)] and acute toxicity were first determined after intraperitoneal administration of G25 in *P. chabaudi*-infected mice (13). Rapid and total clearance of parasites was observed with a 50% effective dose ( $ED_{50}$ ) of 0.08 mg/kg and a 50% lethal dose ( $LD_{50}$ ) of 1.4 mg/kg, indicating a therapeutic index (TI) of 17 in this animal model. These results prompted us to test G25 in vivo against human malaria parasites in *Aotus* monkeys (13). Animals infected with the *P. falciparum* FVO strain (14, 15) generally develop fulminating parasitemia (Fig. 1A, monkey M100) and, if not treated, die with parasitemia above 10 to 20%. Animals were initially treated when parasitemia was  $\sim$ 0.1%, at about 4 days after infection. G25 was administered intramuscularly (i.m.) twice daily for 8 days. Three monkeys treated with 0.2 mg of G25 per kg of body weight (9) were cured 4 days after treatment started and showed no recrudescence at 60 days follow-up (e.g., M151; Fig. 1A). Similar clearance was noted after treatment with quinine (M150, Fig. 1A) and Fansidar (9).

To determine the minimal effective G25 dose, we treated three monkeys with decreasing doses of G25 at 0.1% parasitemia. At G25 doses of 0.09 and 0.03 mg/kg, parasite clearance occurred on day 4 (Fig. 1B), without recrudescence over 60 days. At a dose of 0.01 mg/kg, parasitemia initially decreased but then rose again at day 2.5. At day 7 and beyond, parasitemia was only detectable in thick blood films, suggesting that a dose of 0.01 mg/kg G25 is close to the threshold of therapeutic activity. We determined the  $LD_{50}$  in rats to be 1.4 mg/kg and the maximal tolerable G25 dose under subacute conditions

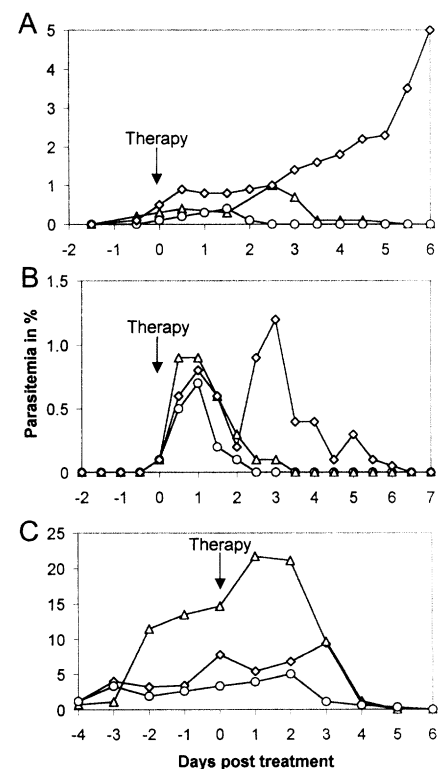
in *Macaca fascicularis* monkeys and beagle dogs to be about 0.9 mg/kg (9). Because *Aotus* monkeys were cured with 0.03 mg/kg, the TI in *P. falciparum*-infected *Aotus* monkeys is at least 30, indicating high in vivo efficacy of G25 against *P. falciparum*. In further experiments, G25 efficacy was tested at about 100-fold higher initial parasitemia (5 to 14%). A total of nine *Aotus* monkeys were treated i.m. with 0.2 mg/kg G25 twice daily over 8 days. Eight monkeys cleared the parasites 4 to 5 days after the first dose (e.g., M169; Fig. 1C) (9), similar to control animals treated with Fansidar (9). One monkey died after 2 days at 19% parasitemia, most likely owing to an irreversible clinical condition. Two monkeys were challenged 60 days after G25 therapy and found to remain susceptible to parasite infection, indicating that parasite clearance and absence of recrudescence were unlikely to be related to antiparasite immunity. Decreasing the G25 dose to 0.09 mg/kg in one monkey (9) or reducing the therapeutic window to only 4 days at 0.2 mg/kg in two monkeys (e.g., V59; Fig. 1C) also successfully cured highly infected monkeys without recrudescence. The permanent cationic charge of G25 did not lead us to expect good oral absorption. Nevertheless, oral administration of G25 at 4 mg/kg over 8 days at 4% initial parasitemia appeared to be fully effective (V51, Fig. 1C). Recent experiments with analogs of G25 designed for good oral bioavailability have shown much higher oral

bioavailability in preliminary experiments in nonhuman primates (16), which is of importance for future first-line antimalarials that must generate oral activity. G25 thus fully succeeded in curing *P. falciparum*-infected monkeys even at high parasitemia without recrudescence.

The other major human malaria parasite, *P. vivax*, favors invasion of immature erythrocytes (reticulocytes). Reticulocytes retain some metabolic activities, which may provide the parasite with compensatory mechanisms under drug pressure. We therefore investigated the activity of G25 against *P. vivax* and against the phylogenetically closely related nonhuman primate parasite *P. cynomolgi* (17), which also favors invasion of reticulocytes. The in vitro  $IC_{50}$  values of G25 against *P. vivax* and *P. cynomolgi* were in the same range as against *P. falciparum* (9), indicating high sensitivity of reticulocyte-restricted parasites to this class of drugs.

For in vivo studies, we used *P. cynomolgi* in rhesus monkeys. G25 treatment was initiated on day 7 after infection when parasitemia ranged between 0.2 and 0.5%. Five monkeys were treated (0.15 mg/kg i.m., twice daily, 8 days), and five remained untreated (Fig. 2). Treated animals had a peak parasitemia of 0.45 to 1% immediately before administration of the second dose (12 hours after treatment). From day 4 onward, parasites were not detectable by thick-film analysis. The five untreated monkeys showed a

**Fig. 1.** In vivo efficacy of G25 against *P. falciparum* in *Aotus* monkeys. *Aotus lemurinus griseimembra* monkeys were inoculated intravenously with  $10^5$  *P. falciparum* FVO-infected RBCs isolated from a donor monkey. Parasitemia was determined by analysis of Giemsa-stained thin films. Antimalarial treatments were started either as soon as patent parasitemia became detectable [generally on day 4 to 6 after infection (A and B)] or later at a higher initial parasitemia (C). The start of therapy was defined as day 0. G25 in saline was administered i.m. at 8 a.m. and 8 p.m. for 8 days. (A) Monkey M151 ( $\circ$ ) was treated with 0.2 mg/kg G25, and M150 ( $\Delta$ ) with a single 30-mg dose of quinine (i.v.). An infected untreated control monkey M100 ( $\diamond$ ) showed typical development with steadily rising parasitemia. M100 was cured on day 7 at 8% parasitemia with a single oral dose of 25 mg/kg Fansidar. (B) The G25 doses were reduced to 0.09 mg/kg (M67,  $\circ$ ), 0.03 mg/kg (M74,  $\Delta$ ), and 0.01 mg/kg (M156,  $\diamond$ ). (C) Representative data from monkeys treated at an initial parasitemia above 5%. G25 was given at doses of 0.2 mg/kg twice daily either for 8 days (M169,  $\diamond$ ) or for only 4 days (V59,  $\Delta$ ); monkey V51 ( $\circ$ ) received oral G25 doses of 4 mg/kg twice daily for 8 days. All animals were tested for parasites up to 60 days after treatment with both Giemsa-stained thick and thin films and a highly sensitive method based on polymerase chain reaction amplification of species-specific sequences from small ribosomal RNA genes, as described (30). All animals remained parasite free.



## REPORTS

typical blood-stage parasitemia development for *P. cynomolgi* M strain in rhesus monkeys (18, 19). A peak parasitemia ranging from 5 to 10% at 3.5 days after the start of treatment was observed, and all control monkeys showed a typical recrudescence (0.2 to 2.5% parasitemia) at day 10 or 11. In contrast, no recrudescence was detected in treated monkeys until the end of the experiment at day 36. At day 3, blood samples obtained from all treated monkeys and from one untreated monkey were washed extensively to remove circulating G25 and cultured overnight to determine whether parasites could recover and develop further in fresh culture medium. Parasites from treated monkeys did not recover, whereas untreated parasites grew well, indicating that G25 toxic activity was irreversible.

G25 thus fulfills essential *in vitro* and *in vivo* criteria for the development of a new class of antimalarials. G25 cured infected monkeys at doses of 0.03 mg/kg, far below those used with current antimalarials (CQ, Q, and mefloquine). The satisfactory TI is lower *in vivo* in the monkey model (>30) than *in vitro* (~2000). This difference is due to a specific interaction of G25 with the cholinergic system. Experiments with rodents indicate that at very high doses, G25 provokes a rapid and transient hypoxia as a result of interference with respiratory muscles, a decrease in the respiration rate, and concomitant strong hemoglobin oxygen desaturation (9). Indeed, the LD<sub>50</sub> could be increased ninefold if G25 was given while providing respiration assistance for the rat (9).

To study the interaction of the effectors with infected erythrocytes, we synthesized the tritium-labeled bisquaternary ammo-

nium salt VB5-T (*N,N,N',N'*-tetramethyl-*N,N'*-di{2-*N*[2-(*p*-<sup>3</sup>H-benzoyl)benzoyl]-aminoethyl}-1,12-dodecanediaminium dibromide) (9). VB5-T is a G25 analog, predicted by our SAR studies and confirmed experimentally to have potent *in vitro* antimalarial activity [IC<sub>50</sub> of 18.3 ± 3.3 nM (SEM, *n* = 4)]. Using enriched *P. falciparum* trophozoite preparations (20), we observed that almost 180-fold more VB5-T was accumulated in infected than in normal red blood cells (RBCs) (1253 ± 108 pmol and 7 ± 1 pmol per 10<sup>10</sup> cells, respectively). We measured drug accumulation (9) at VB5 concentrations ranging between 0.002 and 25 μM after 10-min incubations (Fig. 3A). Accumulation was linear with increasing VB5 concentrations. No saturation was observed around the IC<sub>50</sub> of VB5 (Fig. 3A, inset) or at concentrations up to 1000-fold above the IC<sub>50</sub> of VB5. In a kinetic analysis with 50 nM and 1 μM VB5, accumulation increased linearly over the 3.5-hour time course of the experiment (10). At the same time, the cellular accumulation ratio (CAR), *i.e.*, the concentration ratio of cell-associated VB5 to that in the same volume of culture supernatant, increased linearly to a value of ~300. A steady state was observed only at 25 μM VB5 (plateau at 1600 nmol/10<sup>10</sup> cells after 2 hours) (Fig. 3B). VB5-T accumulation was essentially irreversible; indeed, infected RBCs that had been loaded with VB5, washed, and reincubated in fresh medium retained 95 and 87% of VB5 after 3 hours at 37° and 4°C, respectively (Fig. 3C). Accumulation was not due to a metabolism-dependent concentration gradient. Indeed, high-performance liquid chromatography of infected RBCs loaded for 1 hour at 37°C with 250 nM VB5-T revealed that more than 80% of the total radioactive material eluted at the same retention time as coinjected, nonradioactive

VB5-H preparation (9). Finally, VB5-T is not substantially accumulated in human CD4<sup>+</sup> lymphocytes [CAR of 1.4 and 5.3 after 10 and 60 min, respectively (9)], corroborating the absence of toxicity of G25 in this cell line (9).

Initial fractionation studies with saponin lysis (21) indicated that more than 70% of accumulated VB5-T was recovered in the 100,000g pellets, whereas less than 20% was present in the erythrocyte cytosol fraction; the parasite cytosol appeared to be virtually free of VB5-T (10). VB5-T did not copurify with hemozoin crystals (22), and Ro40-4388, an inhibitor of hemoglobin proteolysis that interferes with the accumulation of the important antimalarial CQ (23), had no effect on VB5 accumulation or on G25 *in vitro* antimalarial activity [at 5 μM Ro40-4388 (10)], indicating that the mode of action of quaternary ammonium salts is likely to be independent of hemoglobin degradation. Furosemide (24), an inhibitor of the parasite-induced new permeation pathway (NPP) (25), had no effect on VB5 accumulation [at 100 μM furosemide (10)], indicating that VB5 accumulation does not involve the NPP. This is in contrast to pentamidine, an antiprotozoal drug of the diamidine compound class (26). Our current hypothesis is that VB5-T accumulates in association with the extensive membrane network surrounding the parasite (27), leading to a concentration of the drug at the parasite surface, where it might interfere with choline uptake and consequent PC synthesis by the parasite.

The *in vivo* properties of anti-PL effectors against human malaria in nonhuman primates indicate that these compounds fulfill many criteria for potential clinical development. The concentration of bisquaternary ammonium salts through accumulation in infected erythrocytes could explain both their potent activity and their specificity for parasitized RBCs.

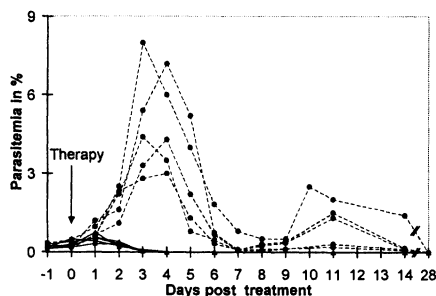


**Fig. 2.** Efficacy of G25 against *P. cynomolgi*-infected rhesus monkeys. An adult *Macaca mulatta* (rhesus) monkey was infected with *P. cynomolgi* M strain blood-stage parasites. At 1% parasitemia, 10<sup>6</sup> parasites were used to infect 10 rhesus monkeys (3 to 6 years of age, sex-matched into two groups of five). At day 7 after infection (parasitemia 0.2 to 0.5%), treatments were started with G25 in saline (*i.m.*, 0.15 mg/kg twice daily, 8 days) (Δ). Control monkeys (●) received saline injections. Parasitemia was determined on finger-prick blood with Giemsa-stained thin and thick blood films.

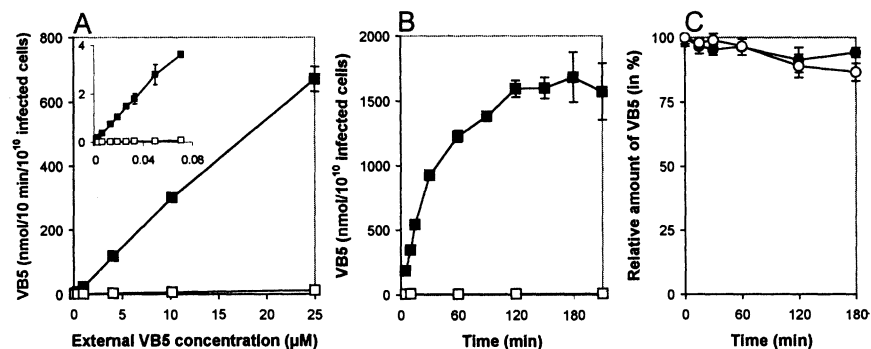


**Fig. 3.** Accumulation of VB5-T in infected erythrocytes. (A) Accumulation of VB5-T in infected (■) and normal RBCs (□) after 10 min at 37°C at a range of external concentrations. (B) Kinetic analysis of VB5 accumulation at 25 μM in infected (■) and normal (□) erythrocytes. (C) Release of VB5-T from infected erythrocytes that had been preloaded for 10 min with 50 nM VB5-T. Cells were washed to remove excess VB5 and reincubated in complete medium either at 37°C (●) or 4°C (○). Quantities of VB5 remaining with the cells were expressed as a percentage of the amount after the wash (time = 0). In all graphs values are the mean ± SD (small SDs are hidden by the symbols) of one representative experiment performed in triplicate. Experiments were repeated twice.

# Midbrain Control of Three-Dimensional Head Orientation

Elia M. Klier, Hongying Wang, Alina G. Constantin, J. Douglas Crawford\*

Little is known about the neural mechanisms controlling head posture and why they fail in clinical syndromes like torticollis. It is well established, however, that the brain controls eye position by integrating eye velocity commands. By electrically stimulating and reversibly inactivating midbrain sites in the head-free (nonimmobilized) monkey, we found that the interstitial nucleus of Cajal functions as a neural integrator for head posture. We suggest that a bilateral imbalance in this structure, through either direct damage or inappropriate input, could be one of the mechanisms underlying torticollis.

The head participates in the control of visual gaze (1, 2) and in several stabilizing/righting reflexes (3, 4). However, some people have a clinical disorder called torticollis (literally meaning "twisted neck") that causes their heads to become locked in inappropriate positions (5, 6). Although these abnormal positions may have various horizontal and vertical components, the head is usually deviated torsionally (i.e., rolled about an axis running between the nose and the back of the head) (6). Unfortunately, little is known about the neural mechanisms of either normal or abnormal head posture. For example, it is not known if head posture is an emergent property of distributed reflex systems or if there is one common path that sets the desired level of neck muscle activation (6).

One clue might be drawn from the oculomotor system, which is closely associated with head control during gaze shifts (1, 7) but is much better understood. Eye orientation is held by a neural integrator that converts velocity-like movement commands into tonic position signals for the eye muscles (8). The pons and medulla have circuitry for horizontal eye velocity integration (9), whereas the midbrain interstitial nucleus of Cajal (INC) participates in integrating vertical and torsional eye movement signals, with clockwise (CW) and counterclockwise (CCW) torsion controlled on opposite sides of the midline (10, 11). Anatomical and physiological evidence also implicate the INC in the control of head motion because some of its output neurons participate in the interstitio-spinal tract, which controls neck muscles (12). Thus, the INC might also have a neural integrator for head control (13, 14).

We recorded three-dimensional (3D) orientations of the eye and head in four alert and behaving monkeys (*Macaca fascicularis*) (15, 16). The 3D motor behavior and brainstem physiology of these monkeys are nearly identical to that of humans (17, 18). Electrical stimulations were delivered to the INC and surrounding regions during periods of motionless gaze fixation (19). In all, 93 putative INC sites were stimulated in monkey 1 (M1), 19 sites in M2, 9 sites in M3, and 8 sites in M4 in light, dim light, and complete darkness.

Figure 1 shows simulated head caricatures accurately depicting final 3D head orientations measured after stimulations in either the left or right INC. These stimulations produced mainly torsional deviations in head position, with final head postures resembling those seen in torticollis. The same stimulations produced small or variable vertical movements (perhaps because up and down vertical signals are intermingled in the INC so that they cancel during stimulation) and even smaller systematic horizontal movements (Fig. 1, B and C). Stimulation of the right side (from midline) always produced CW rotations of the head (77 sites), whereas leftward stimulations always produced CCW head rotations (52 sites), from the subject's viewpoint (20).

These observations suggest that the INC is involved in the active control of head orientation. To understand the nature of its control signals, we looked at the time course of the evoked torsional movements (Fig. 1, B and C). These trajectories initially showed a delayed and sluggish response after stimulation onset, as expected with a high-inertia system like the head. But once in motion, the head moved with a constant velocity "ramp" until stimulation offset. Then, after a brief delay, the head stopped moving and held all or most of its induced torsional position (21). This is the sort of time course expected if one charges up an integrator with a constant input and then

## References and Notes

1. P. A. Winstanley, *Parasitol. Today* **16**, 146 (2000).
2. H. Vial, M. L. Ancelin, in *Malaria: Parasite Biology, Pathogenesis, Protection*, I. W. Sherman, Ed. (American Society for Microbiology, Washington, DC, 1998), pp. 159–175.
3. L. L. M. Van Deenen, in *The Red Blood Cell*, G. Surgenor, Ed. (Academic Press, New York, 1975), pp. 147–211.
4. M. Calas *et al.*, *J. Med. Chem.* **40**, 3557 (1997).
5. M. L. Ancelin *et al.*, *Blood* **91**, 1426 (1998).
6. H. J. Vial *et al.*, in *Transport and Trafficking in the Malaria-Infected Erythrocyte* (Novartis Foundation Symposium 226, Wiley, Chichester, UK, 1999), pp. 74–88.
7. M. Calas *et al.*, *J. Med. Chem.* **43**, 505 (2000).
8. *P. falciparum* was maintained under standard conditions (28) with human O<sup>+</sup> erythrocytes in complete medium (RPMI 1640 medium with 10% human AB<sup>+</sup> serum and 40 µg/ml gentamicin). Human cell lines were cultured as described (29).
9. Supplementary material showing in vitro G25 activities, all data on G25-treated monkeys, detailed G25 clinical effects, animal study protocols, VB5 accumulation assays, and the chemical syntheses of VB5-T and VB5-H are available on Science Online at [www.sciencemag.org/cgi/content/full/295/5558/1311/DC1](http://www.sciencemag.org/cgi/content/full/295/5558/1311/DC1).
10. H. J. Vial *et al.*, data not shown.
11. B. N. Ames, J. McCann, E. Yamasaki, *Mutat. Res.* **31**, 347 (1975). The tests were performed at the Istituto di Ricerche Biomediche "Antoine Marxer," Italy.
12. W. Peters, *Chemotherapy and Drug Resistance in Malaria* (Academic Press, New York, 1970).
13. All animal study protocols were performed in accordance with legislative guidelines (9). All nonhuman primate study protocols were evaluated and approved by independent animal care and use committees before the beginning of the studies.
14. C. C. Campbell, W. Chin, W. E. Collins, S. M. Teutsch, D. M. Moss, *Lancet* **2**, 1151 (1979).
15. S. Herrera *et al.*, *Proc. Natl. Acad. Sci. U.S.A.* **87**, 4017 (1990).
16. H. Vial, A. Thomas, unpublished data.
17. C. H. Kocken, A. van der Wel, B. Rosenwirth, A. W. Thomas, *Exp. Parasitol.* **84**, 439 (1996).
18. G. R. Coatney, W. E. Collins, W. McWarren, P. G. Contacos, *The Primate Malarial* (U.S. Government Printing Office, Washington, DC, 1971).
19. C. Kocken, A. Thomas, unpublished observation.
20. S. Kutner, W. V. Breuer, H. Ginsburg, S. B. Aley, Z. I. Cabantchik, *J. Cell. Physiol.* **125**, 521 (1985).
21. B. D. Beaumelle, H. J. Vial, J. R. Philippot, *J. Parasitol.* **73**, 743 (1987).
22. D. J. Sullivan Jr. *et al.*, *Proc. Natl. Acad. Sci. U.S.A.* **93**, 11865 (1996).
23. P. G. Bray, M. Mungthin, R. G. Ridley, S. A. Ward, *Mol. Pharmacol.* **54**, 170 (1998).
24. K. Kirk, *Physiol. Rev.* **81**, 495 (2001).
25. ———, H. A. Horner, B. C. Elford, J. C. Ellory, C. I. Newbold, *J. Biol. Chem.* **269**, 3339 (1994).
26. A. M. Stead *et al.*, *Mol. Pharmacol.* **59**, 1298 (2001).
27. L. H. Bannister, J. M. Hopkins, R. E. Fowler, S. Krishna, G. H. Mitchell, *Parasitol. Today* **16**, 427 (2000).
28. W. Trager, J. B. Jensen, *Science* **193**, 673 (1976).
29. C. Gumila *et al.*, *Antimicrob. Agents Chemother.* **40**, 602 (1996).
30. G. Snounou, S. Viriyakosol, W. Jarra, S. Thaithong, K. N. Brown, *Mol. Biochem. Parasitol.* **58**, 283 (1993).
31. We are grateful to J. C. Doury, P. Ringwald, L. Basco, J. Le Bras, D. Warhurst, the World Health Organization (WHO), and the Walter Reed Army Institute of Research for testing the compounds in their laboratories. We thank A. van der Wel, M. Dubbed, and S. Rivière for technical assistance and C. Ben Mamoun and R. G. Ridley for critical reading of the manuscript. These studies were supported by grants from the European Union (INCO-DEV, IC18-CT960056, QLK2-CT-2000-01166), CNRS-Direction Générale de l'Armement (GDR 1077), Ministère de l'Éducation Nationale, de la Recherche et de la Technologie (PRFMMIP and VIHPAL), and the U.N. Development Bank–World Bank–WHO special program for Research and Training in Tropical Diseases. K.W. is supported by a Marie Curie fellowship of the European Union.

18 October 2001; accepted 4 January 2002

CIHR Group for Action and Perception, York Centre for Vision Research and Departments of Psychology, Biology and Kinesiology & Health Sciences, York University, Toronto, Ontario M3J 1P3, Canada.

\*To whom correspondence should be addressed. E-mail: [jdc@yorku.ca](mailto:jdc@yorku.ca)